Ultrahigh Frequency Nanotube Resonators

H. B. Peng, C. W. Chang, S. Aloni, T. D. Yuzvinsky, and A. Zettl

Department of Physics and Center of Integrated Nanomechanical Systems, University of California at Berkeley, and Materials Sciences Division, Lawrence Berkeley National Laboratory, Berkeley, California 94720, USA

(Received 17 January 2006; published 22 August 2006)

We report carbon-nanotube-based electromechanical resonators with the fundamental mode frequency over 1.3 GHz, operated in air at room temperature. A new combination of drive and detection methods allows for unprecedented measurement of both oscillation amplitude and phase and elucidates the relative mobility of static charges near the nanotube. The resonator serves as an exceptionally sensitive mass detector capable of $\sim 10^{-18}$ g resolution.

DOI: 10.1103/PhysRevLett.97.087203 PACS numbers: 85.85.+j, 73.63.Fg, 74.78.Na, 81.16.Rf

Nanoelectromechanical systems (NEMS) [1–8] are becoming ever more important for fundamental research and technical applications. Of special interest is the high-frequency NEMS resonator [2,3,6–8], which not only offers the potential for extreme mass and force sensitivity [7] but also provides a unique way to observe the imprint of quantum phenomena directly [2], including uncertainty-principle limits on position detection [6]. Various bottom-up (self-assembly) and top-down (lithographical) fabrication processes have been employed to create NEMS devices, but none has achieved the ''holy grail'' of ultrahigh-frequency (>1 GHz) operation at room temperature in atmospheric pressure. In the case of doubly clamped beam resonators, the highest resonance frequency, 1.029 GHz, was reported in devices made of stiff 3C-SiC beams, with motion detectable at a temperature of 4.2 K [8]. On the other hand, carbon nanotubes (CNTs) [9–12] have been considered promising candidates for NEMS resonators. Recently [13], electrical detection of mechanical resonance of doubly clamped suspended CNTs was demonstrated, although the frequencies were below 200 MHz, and no resonance was detectable at atmospheric pressure.

Here we present suspended CNT-based resonators with the fundamental mode frequency over 1.3 GHz and mechanical motion self-detectable at room temperature in air at atmospheric pressure. A new combination of drive and detection methods, along with metal nanobridges templated onto the CNT beam, are used to dramatically enhance the response sensitivity (including phase response) and to probe mobility of trapped charges of the NEMS device. Extreme mass sensitivity of the resonators is clearly demonstrated.

Figure 1(a) gives a schematic cross-sectional view of our doubly clamped CNT resonator with a local gate. The suspended CNT devices were fabricated according to a process described previously [14,15]. Two head-on source-drain electrodes (Pt 20 nm/Cr 5 nm), with a thin layer of Fe on top as a catalyst, were patterned by *e*-beam lithography on Si_3N_4(50 nm)/SiO_2(500 nm)/Si substrates. The gap between the source and drain electrodes was typically from 300 nm to 1 μm. After this, a second *e*-beam lithography step, reactive ion etching, and buffered HF etching were carried out to pattern a trench between the source and drain electrodes, with the trench depth typically between 200 and 500 nm. A successive evaporation of Pt 20 nm/Cr 5 nm and then a lift-off process finalized a local gate on the bottom of the trench [16]. Subsequently

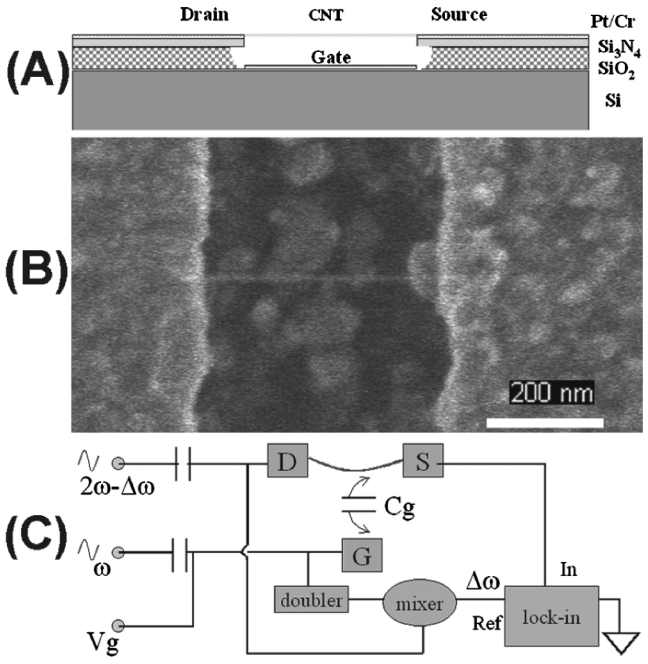

FIG. 1. (a) Schematic cross section of the CNT resonator. (b) SEM image of a suspended CVD-grown carbon nanotube crossing a trench. Scale bar: 200 nm. (c) Schematic experimental diagram for the 2ω method. An actuation rf signal of amplitude δV_g at frequency ω is applied to the gate, together with a dc bias V_g. A carrier rf signal of amplitude δV_d is applied to the drain at frequency 2ω-$\Delta\omega$. The ac current flow through the source at the frequency $\Delta\omega$ is monitored using a lock-in amplifier with a time constant 300 ms. The lock-in reference at the frequency $\Delta\omega$ is obtained through a frequency doubler and a mixer.

suspended single-wall CNTs were grown by chemical vapor deposition (CVD) [14,15,17] directly across the trenches, thereby electrically bridging the source and the drain. Figure 1(b) gives a scanning electron microscope (SEM) image of a device with a suspended CNT. Such devices could be operated either with bare CNTs or with nanobridges created by coating the CNTs via a further step of thermal evaporation of metals.

Two methods were used to drive and electrically detect the mechanical oscillations of the NEMS resonators. In the first, termed the "1ω" method [13], an actuation rf signal is applied to the gate at frequency ω and a carrier signal is applied to the drain at a slightly different frequency ω-$\Delta\omega$. The drain-source current is monitored by a lock-in amplifier at the intermediate frequency $\Delta\omega$, and the nanotube serves as a mixer. In our newly implemented "2ω" method, the actuation signal applied to the gate is at frequency ω, while the carrier signal applied to the drain is at frequency 2ω-$\Delta\omega$, instead of ω-$\Delta\omega$. The electrical current flow through the resonator is monitored at the intermediate frequency $\Delta\omega$ ($\sim$7 KHz) again by lock-in techniques. When the oscillator is driven through resonance, a sharp change occurs in both the amplitude and the phase of the measured ac electrical current. Figure 1(c) illustrates the experimental setup for the 2ω method. The frequency doubling of the driving force results from the fact that the electrostatic force on a capacitor is proportional to the square of the voltage-induced charge [18].

Figure 2 shows the amplitude and phase response for a CNT-based NEMS resonator obtained at room temperature. This particular resonator has a metal nanobridge coating, and the detection method is 1ω. When the resonator is operated in a low pressure environment ($\sim 10^{-6}$ Torr, solid triangles), a well-defined fundamental resonance is clearly observed at 1.33 GHz. When the resonator is operated in air at atmospheric pressure (hollow circles), the resonance is qualitatively similar in amplitude and phase but the resonance frequency has shifted slightly downward to 1.32 GHz. The observed shift is attributable to the adsorption of air-specific molecules (such as water and oxygen) around the CNT, leading to a change of the resonator mass.

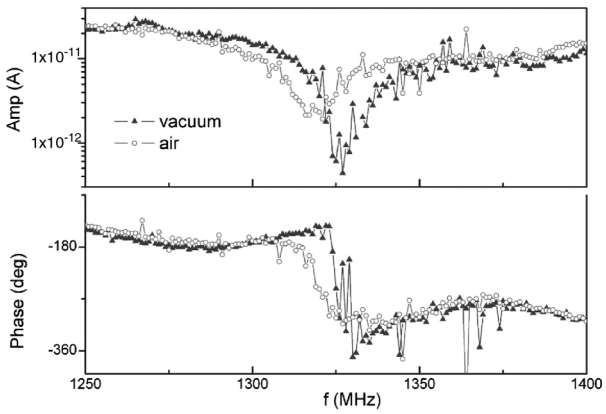

FIG. 2. Amplitude (in logarithmic scale) and phase of the electrical current in a vacuum $\sim 10^{-6}$ Torr (triangles) and in air (circles) for a nanobridge resonator made from coating a bare suspended CNT device with 2.5 nm indium. The data were taken at $V_g = 0$, $\delta V_g = 112$ mV, and $\delta V_d = 46$ mV by the 1ω method.

As expected, resonators with a shorter clamping CNT length generally have higher fundamental resonance frequencies. The highest resonance frequency we have observed is 1.85 GHz using a trench width of 300 nm. However, the observed resonance frequency varies even between devices with the same trench width, a consequence of different CNT diameter, CNT defect density, and effective clamping strength (which influences the effective clamping length).

We now explore details of the resonator response. Figure 3 shows the amplitude and phase for a bare CNT resonator operated at room temperature. The star symbol data are measured by the 1ω method; i.e., the rf signal applied to the gate is at the same frequency as the effective driving frequency ω. The current amplitude [Fig. 3(a)]

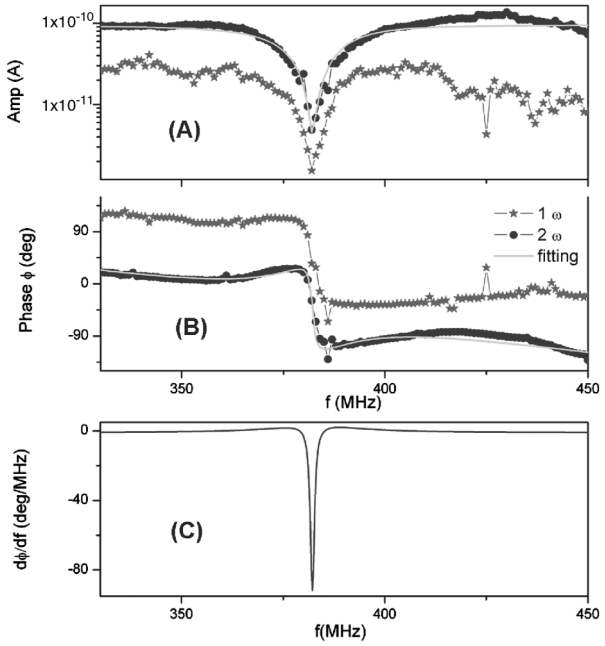

FIG. 3. Amplitude in logarithmic scale (a) and phase (b) of current response as a function of effective driving frequency f for a bare CNT resonator, taken with $V_g = 0$, $\delta V_g = 158$ mV, and $\delta V_d = 70$ mV by the 1ω method (star) and the 2ω method (circle) at room temperature in a vacuum $\sim 3 \times 10^{-6}$ Torr. The solid lines (gray) in (a) and (b) are the fitting results according to the theory described in the text, with $Q = 15$, $\omega_0/2\pi = 382.7$ MHz, and $\phi_b = -92.25°$. [Experimentally, the cable length difference of the reference and the input of the lock-in induced a linearly varying phase with respect to frequency ($\sim 0.99°/\text{MHz}$), which was added to the total phase ϕ in Eq. (1) in the fitting.] The derivative of phase with respect to the effective driving frequency $d\phi/df$ for the fitted data is shown in (c).

shows a sharp decrease by more than an order of magnitude at 382 MHz with a concomitant abrupt change of the measured phase [Fig. 3(b)]. Presented also in Fig. 3 (solid circle) is the response measured using the 2ω method; i.e., the rf signal at the gate electrode is set at half of the effective driving frequency. The 2ω method gives a cleaner signal with a resonance frequency identical to that from the 1ω method and yields a significantly stronger current amplitude than the 1ω method.

The observed resonator response can be analyzed to elucidate fundamental physics of the nanotube-based NEMS resonators. Importantly, the combination of the 1ω and 2ω methods can be exploited to gain insight into the distribution and mobility of excess accumulated charges, which are inevitable to nanoscale systems. The relative strength of the 1ω and 2ω response depends on the amount and mobility of excess accumulated charges on the resonator [18]. For some samples, such as the one shown in Fig. 3, there was no significant difference in the relative strength of the 1ω and 2ω signals as we experimentally varied the dc gate bias V_g. Hence, we conclude that for such devices the static charges (induced by V_g) are likely trapped in defect states and have low mobility. For some other devices, the 2ω response is much stronger at zero dc gate bias, but the 1ω component increases and eventually dominates as dc gate bias V_g is increased. In those cases, we conclude that the dc gate bias induces static charges which are mobile enough to be modulated by the rf gate actuation signal.

The overall electrical response can be ascribed to the interference of a background response and a resonance response due to the mechanical motion [3,13,19]. The background response is the signal induced by the rf gate voltage even if the resonator beam has no mechanical motion, e.g., the signal due to the field effect. The resonance response is the conductance change due to the mechanical resonant motion, which, in general, includes any strain effect and the extra field effect (e.g., resulting from a motion-induced capacitance change). Hence, we express the measured current response as

$$Ie^{i\phi} = I_b e^{i\phi_b} + I_r e^{i\phi_r}, \tag{1}$$

where I, I_b, and I_r are the amplitudes of the measured total current, the background current, and resonance-induced current, respectively, while ϕ, ϕ_b, and ϕ_r are the corresponding phases. We employ Euler-Bernoulli theory for doubly clamped beams [20], whereby the resonance-induced signal due to the fundamental mode is given by

$$I_r e^{i\phi_r} = \frac{c}{\omega_0^2 - \omega^2 - i\omega_0^2/Q}, \tag{2}$$

where w_0 is the resonance frequency, Q is the quality factor, and c is a parameter independent of the frequency ω. The background amplitude and the phase are usually treated as constants within the considered frequency range. The fitting curve in Figs. 3(a) and 3(b) represents Eq. (1) with resonance frequency $\omega_0/2\pi = 382.7$ MHz and quality factor $Q = 15$ [21]. Note that in Eq. (2) we use a minus sign in the term containing the Q factor, which is different from the expression in Ref. [20] but is crucial for fitting the experimental data of the phase response correctly. Therefore, the physical origin of Eq. (2) implies that the unrelaxed Young's modulus (the high-frequency limit) is less than the relaxed modulus (the low-frequency limit) for carbon nanotubes according to Zener's model [20].

It is interesting that, due to the interference between the background and the resonance response, the phase signal reveals an abrupt transition near the resonance [changing by $\sim 110°$ within 3 MHz in Fig. 3(b)], much sharper than that of a pure Lorentzian signal with the same Q factor. The derivative of the phase, as shown in Fig. 3(c), gives a full width at half maximum of ~ 1.2 MHz, leading to an effective "phase quality factor" $Q_p = 320$. (A similar analysis of the 1.3 GHz resonance of Fig. 2 finds $Q_p = 440$.) We therefore obtain an enhanced quality factor in the phase signal, which may offer a great advantage in detecting the frequency shift for sensing applications. (Experimentally, the observed abrupt phase change is well reproducible. However, we acknowledge that a rigorous theoretical investigation of the signal to noise ratio can be very helpful for future practical applications using the enhanced phase response.) Note that, for a Duffing resonator, a strong nonlinear effect could also result in an abrupt phase response [22–25]. Under high drive power above a critical value, bifurcation can occur, and a hysteric response results with abrupt changes in both amplitude and phase upon different sweeping directions. However, the absence of frequency sweep hysteresis and drive-power-independent sharp phase changes indicate that our measurements are performed in the linear region.

The resonator frequency and geometry allow the CNT elastic modulus to be determined. With the CNT being modeled as a thin-wall cylinder, the fundamental frequency is given by $\omega_0/2\pi = 1.259\sqrt{E/\rho}(d/L^2)$, where E is the Young's modulus, ρ is the density, d is the diameter, and L is the length of the doubly clamped CNT. With $L = 300$ nm, $d = 3.5$ nm, $\rho = 1.3$ g/cm^3, and $\omega_0/2\pi = 382.7$ MHz relevant for the device of Fig. 3, we obtain $E = 80$ Gpa for the CNT Young's modulus. Our value of E is a lower limit [9], in light of the "softness" of the clamping at the trench edges and a consequent underestimation of the effective nanotube length L.

Of great current interest is the possibility of employing NEMS resonators as mass detectors, and the exceptionally low intrinsic mass of CNTs suggests their use in an extreme (molecular-level) mass sensitivity configuration [10]. Figure 4 presents the electrical response of a CNT Fe-bridge device before and after receiving a small amount of Fe mass loading by thermal evaporation. Prior to mass

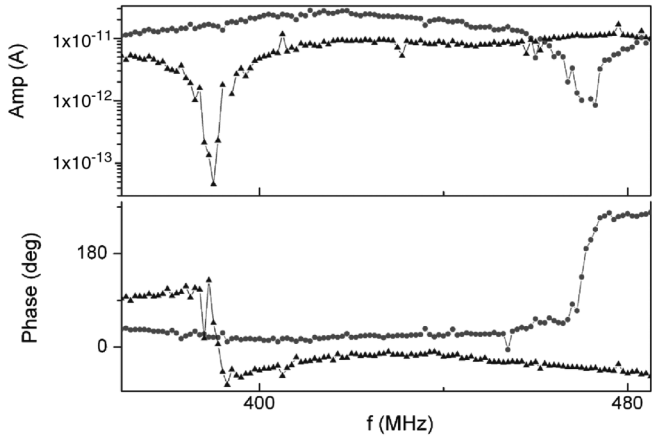

FIG. 4. Electrical response (with amplitude in logarithmic scale) of a Fe-coated nanobridge resonator (circle) and the same device after an additional loading of 2 nm Fe (triangle), measured with $V_g = 0$ and $\delta V_g = 21$ mV by the 1ω method.

loading, the resonance frequency is 470 MHz (circles), while, after 2 nm of Fe have been deposited onto the CNT beam (measured by a quartz crystal monitor), the resonance is shifted downward to 390 MHz (triangles). Assuming that the mass loading results in a 2 nm Fe coating over a cross-sectional area 2220 nm^2 (the projected beam area for this resonator), we obtain a rough estimate for the added mass of $\sim 3.5 \times 10^{-17}$ g. With the frequency shift proportional to the added mass [7], from the phase signal we have a detectable mass sensitivity of $\sim 10^{-18}$ g with $\delta\omega = 3$ MHz (associated with an experimentally observed phase change of 140° near resonance for the nanobridge resonator before the mass loading). From the amplitude data, a lower-bound mass sensitivity can be estimated as $\sim 7 \times 10^{-18}$ g by taking $\delta\omega =$ 16 MHz, the full width of the half depth of the resonance response. We note that there is a sign change of the phase shift in the response between the unloaded and the loaded resonators. This can be well explained within the interference model by a slight change of the magnitude of the pure resonance signal from a value larger than the background signal magnitude to a value smaller than the background signal magnitude.

In summary, resonance frequencies over 1.3 GHz have been realized with CNT-based NEMS resonators. A new combination of 1ω and 2ω mixing methods allows for unprecedented measurement of both oscillation amplitude and phase and elucidates the relative mobility of static charges. Further scaling down CNT-based resonators and selecting suitable coating materials may achieve extremely high resonance frequencies over 10 GHz or even into the terahertz range. Moreover, using as-grown suspended CNTs as templates may open new ways to fabricate a variety of NEMS devices beyond the reach of current standard lithography. We expect that the self-detecting gigahertz resonators will pave the way for practical applications, as well as provide model systems for quantum measurements [2].

We thank K. Jensen and B. Kessler for helpful interactions. This work was supported in part by NSF Grant No. EEC-0425914 and by DOE Contract No. DE-AC-03-76SF00098.

[1] H. G. Craighead, Science **290**, 1532 (2000).
[2] K. C. Schwab and M. L. Roukes, Phys. Today **58**, No. 7, 36 (2005).
[3] R. G. Knobel and A. N. Cleland, Nature (London) **424**, 291 (2003).
[4] A. F. Fennimore *et al.*, Nature (London) **424**, 408 (2003).
[5] D. Rugar *et al.*, Nature (London) **430**, 329 (2004).
[6] M. D. LaHaye *et al.*, Science **304**, 74 (2004).
[7] K. L. Ekinci and M. L. Roukes, Rev. Sci. Instrum. **76**, 061101 (2005).
[8] X. M. H. Huang *et al.*, Nature (London) **421**, 496 (2003); for blade-geometry resonators, the highest fundamental frequency reported is 1.1 GHz; see V. Agache *et al.*, Appl. Phys. Lett. **86**, 213104 (2005).
[9] *Carbon Nanotubes: Synthesis, Structure, Properties, and Applications*, edited by M. S. Dresselhaus, G. Dresselhaus, and P. Avouris (Springer, Berlin, 2001).
[10] P. Poncharal *et al.*, Science **283**, 1513 (1999).
[11] S. T. Purcell *et al.*, Phys. Rev. Lett. **89**, 276103 (2002).
[12] B. Babić *et al.*, Nano Lett. **3**, 1577 (2003).
[13] V. Sazonova *et al.*, Nature (London) **431**, 284 (2004).
[14] H. B. Peng *et al.*, Appl. Phys. Lett. **83**, 4238 (2003).
[15] H. B. Peng and J. A. Golovchenko, Appl. Phys. Lett. **84**, 5428 (2004).
[16] J. Cao *et al.*, Small **1**, 138 (2005).
[17] A preconditioning method was adopted from N. R. Franklin and H. Dai, Adv. Mater. **12**, 890 (2000).
[18] Details of the 2ω method will be published elsewhere.
[19] The conductance change due to the electrostatic force on a CNT can result from field effect, strain effects along the CNT and at the contacts, and possible resonant heating. The fact that we are able to obtain similar results for semiconducting and metallic CNTs suggests that strain effects dominate the transduction process.
[20] A. N. Cleland and M. L. Roukes, J. Appl. Phys. **92**, 2758 (2002).
[21] We note that, for the best fit of Eq. (1) to the data presented in Fig. 3, $I_b/I_r \approx 1$ and $\phi_b \approx -\pi/2$. These "coincidental" fitting parameters are not universal; as expected, for some other resonators (experimentally also showing sharp current amplitude reduction and sharp phase changes near resonance), I_b/I_r and ϕ_b extracted from best fits to the interference model are different.
[22] I. Siddiqi *et al.*, Phys. Rev. Lett. **94**, 027005 (2005).
[23] J. S. Aldridge and A. N. Cleland, Phys. Rev. Lett. **94**, 156403 (2005).
[24] B. Yurke, D. S. Greywall, A. N. Pargellis, and P. A. Busch, Phys. Rev. A **51**, 4211 (1995).
[25] M. Dykman and M. Krivoglaz, Sov. Phys. JETP **50**, 30 (1979).